Taylor & Francis
Taylor & Francis Group

MOLECULAR &
CELLULAR BIOLOGY

Measurement of altered APP isoform expression in adipose tissue of diet-induced obese mice by absolute quantitative real-time PCR

Hansol Min[a]*, Jinil Kim[a]*, Young-Jin Kim[b], Mi-Sook Yoon[c], Richard E. Pratley[d] and Yong-Ho Lee[a]

[a]Department of Biomedical Science, Catholic University of Daegu, Gyeongsan, Korea; [b]Department of Biomedical Engineering, Catholic University of Daegu, Gyeongsan, Korea; [c]Division of Beauty Coordination, Keimyung College University, Daegu, Korea; [d]Florida Hospital Sanford/Burnham Translational Research Institute for Metabolism and Diabetes, Orlando, FL, USA

ABSTRACT

Obesity is associated with increased risk of Alzheimer's disease. Previous studies have demonstrated that amyloid-beta precursor protein (APP) is expressed in subcutaneous adipose tissue (SAT), upregulated with obesity, and correlates with insulin resistance and adipose tissue inflammation. APP is alternatively spliced into several isoforms, which may be indicative of the pathogenesis of APP-related diseases, but the accurate quantification has been difficult to standardize and reproduce. In light of this, we developed isoform-specific absolute cDNA standards for absolute quantitative real-time PCR (AQ-PCR), and measured transcript copy numbers for three major APP isoforms (APP770, APP751, and APP695), in SAT from C57BL/6 mice fed either a normal or high-fat diet. Expression of all three major APP isoforms was increased in diet-induced obese mice. Transcript copy numbers of APP770 and APP695 correlated with plasma insulin and CCL2 gene expression. The ratios of APP770 and APP751 to APP695 gradually decreased with aging, and correlated with plasma glucose levels. In addition, APP770 was significantly decreased in thiazolidinedione-treated mice. We describe quantification of APP isoform transcripts by AQ-PCR, which allows for direct comparison of gene copy number across isoforms, between experiments, and across studies conducted by independent research groups, which relative quantitative PCR does not allow. Our results suggest a possible role of differential expression of APP isoforms in the development of obesity-related insulin resistance and adipose tissue inflammation. In addition, it is important to determine if altered ratios of APP isoforms in SAT contribute to higher circulating Aβ peptides and increased risk of abnormalities in obesity.

Introduction

A hallmark pathological finding in Alzheimer's disease (AD) was the presence of plaques in the central nervous system that contained insoluble amyloid-β peptide (Aβ), resulting from proteolytic processing of amyloid-beta precursor protein (APP) (Hardy & Selkoe 2002). Although a great deal is known about the regulation of APP expression in the central nervous system, less is known about the regulation of APP expression, processing, and function in peripheral tissues. In previous gene expression studies with GeneChip® microarrays, we have demonstrated that APP mRNA expression was higher in subcutaneous adipose tissue (SAT)/adipocytes and preadipocytes from obese subjects (Lee et al. 2005; Nair et al. 2005; Lee et al. 2008). APP expression in adipocytes and SAT correlated with *in vivo* indices of insulin resistance, the expression of proinflammatory genes,

and Aβ plasma levels (Lee et al. 2008; Lee et al. 2009). We recently demonstrated that similar cellular mechanisms for production and effects of Aβ may exist between neuronal dysfunction in AD and adipose dysfunction in type 2 diabetes (Tharp et al. 2016). In addition to these human studies, we have demonstrated that SAT APP mRNA expression levels were increased in diet-induced obese mice and correlated with indices of glucose metabolism and insulin resistance (Jeong et al. 2014).

APP is alternatively spliced into several mRNA isoforms in a tissue-specific manner. Each isoform can undergo processing to produce several peptide products in addition to Aβ, each with multiple possible functions (Ling et al. 2003). The three major isoforms of APP (APP770, APP751, and APP695) are derived from alternative splicing that removes exon(s) 7 and/or 8; APP770 contains both, APP751 does not contain

exon 8, and APP695 lacks exons 7 and 8. The APP751 and APP770 isoforms contain a 56-amino-acid Kunitz-type protease inhibitor (KPI) domain, whereas APP695 lacks this region (Zhao et al. 2015). APP695 has been described as the neuronally-predominant isoform. APP770 is widely expressed in peripheral tissues, but minimally in CNS tissue.

Several groups have documented variation in APP isoform expression in multiple regions of the brain affected by AD. Although APP695 is the abundant isoform in the human brain, KPI-containing APP (APP-KPI) mRNA levels correlated with Aβ levels and the ratio of APP-KPI protein levels to total APP protein increased in AD (Matsui et al. 2007). Other data have also shown that the amount of APP-KPI increases in the brain of patients with AD and is related to amyloid fibril formation in AD (Barrachina et al. 2005). These results indicate that altered transcription of APP isoforms in AD is associated with Aβ peptides and contribute to Aβ deposition in AD.

Relative quantitative real-time PCR (qPCR) uses a standard curve in which unknown concentrations of RNA or cDNA are used as references for the curve. Since resulting values are arbitrary and unit-less, they can only be compared between samples for gene or isoform expression, but not for same-sample measurement of different genes or isoforms. Therefore, an absolute quantitative method was required for measuring transcript copy number for each APP isoform. Absolute quantitation was achieved by absolute quantitative real-time PCR (AQ-PCR), in which a standard curve was created for each gene, using known concentrations of reference cDNA. Once the exact transcript copy number of one isoform for one sample was obtained, it could then be compared to the copy number of another isoform in the same or another sample. By AQ-PCR in a previous human study, we developed a set of isoform-specific absolute quantitative standards that allow for the quantification of transcript copy numbers for human APP isoforms, and examined expression patterns in brain samples from 12 patients with AD and 10 control subjects (Tharp et al. 2012).

In the current study, we developed a set of PCR primers to produce absolute quantitative standard curves for measuring the three major APP isoforms and GAPDH in mice. We also designed primers and probe sets for real-time PCR in conjunction with our isoform-specific standards to measure APP isoform transcript levels in mouse adipose tissue. We measured transcript copy number for each APP isoform and analyzed whether the expression levels were altered by long-term high-fat diet (HFD) feeding, and correlated these values with indices of glucose metabolism and insulin sensitivity.

Materials and methods

Preparation of mouse APP isoform-specific standards for AQ-PCR

To create mouse APP isoform-specific standard curves, each isoform-specific DNA fragment was amplified and isolated from the corresponding cDNA. PCR primer pairs were designed to amplify isoform-specific transcripts for APP770, APP751, or APP695, and GAPDH from cDNA libraries. Primers for each standard were prepared to produce cDNAs with sequences encompassing the target amplicon as measured by real-time PCR. Testing of empiric combinations yielded pairs of specific primers (Table 1) which produced standards of known size that could be resolved by agarose gel electrophoresis. A standard sample of each isoform and GAPDH was isolated by gel electrophoresis and purified using the QIAquick Gel Extraction kit (Qiagen, Valencia, CA), and re-amplified. Direct sequencing of the amplified standards confirmed that the proper sequence had been amplified (Macrogen, Korea). The weight/volume concentration of the standard samples was determined by spectrometry, and converted to standard copy number/volume by dividing by the molecular weight and multiplying by Avogadro's number. A standard curve with known standard copy numbers for each isoform was made by serial dilution. The cDNA standards for APP770, APP751, APP695, and GAPDH are 261, 193, 143, and 202-bp long, respectively (Table 1).

Animals

The protocols used in this study were reviewed and approved by the Animal Experimentation and Ethics Committee of the Catholic University of Daegu (Gyeongsan, South Korea). A total of 103 C57/BL/6 male mice were used in this study, with 7–10 mice in each group. Blood and abdominal SAT samples were obtained from mice sacrificed at various time points after feeding a normal diet (ND) or a HFD from the age of 6 weeks until the age of 16, 26, 36, 47, or 77 weeks (Jeong et al. 2014; Kim et al. 2014). In addition, blood and tissue samples were collected from obese mice with increased insulin sensitivity by thiazolidinedione (TZD) treatment. Blood samples collected by cardiac puncture from sacrificed mice were centrifuged at $2400 \times g$ for 15 min at 4°C, and the plasma obtained was additionally centrifuged at $12{,}500 \times g$ for 15 min. Non-fasting plasma concentrations of glucose and insulin were measured by glucometer and enzyme-linked immunosorbent assay (ALPCO Diagnostic, Salem, NH), respectively (Jeong et al. 2014; Kim et al. 2014).

Table 1. Primer sequences for amplifying cDNA standards for absolute quantitative real-time PCR.

	Reference sequence	Amplicon size (bp)	Forward primer sequence[a]	Reverse primer sequence[a]
APP770	NM_001198823	261	ccattcttttacggcggatgt	ctttgggttgacacgctg
APP751	NM_001198824	193	agtccgtggaggaggtggtc	gctgtcgtgggaaacacgct
APP695	NM_007471	143	aggtggtccgagttccca	gataacggccttcttgtcag
GAPDH	NM_001289726	202	aatgtgtccgtcgtggatc	Tgtcattgagagcaatgccag

[a]All sequences are listed from 5′ to 3′.

Extraction of RNA and preparation of cDNA from tissue samples

RNA was extracted from SAT samples, using the RNeasy Lipid Tissue Mini kit (Qiagen). During the extraction, RNA was treated with DNase I (Qiagen) to minimize potentially contaminating genomic DNA. A cDNA library was made using the High Capacity cDNA Reverse Transcription kit (Applied Biosystems, Foster City, CA) from 1 μg total RNA, according to manufacturer's instructions. Using relative real-time PCR (qPCR) with synthesized cDNA, the gene expression levels of IL-6, TNFα, and CCL2 in SAT were measured and normalized to that of GAPDH (Jeong et al. 2014).

Absolute quantitative real-time PCR

Custom TaqMan® gene expression assays for AQ-PCR were designed specifically for each APP isoform and GAPDH (Table 2, Figure 1; please also see supplemental Figure S1), and ordered from Applied Biosystems (Applied Biosystems® Custom Primers & TaqMan® Probes). AQ-PCR was carried out using amplified standards and custom TaqMan® gene expression assays on a StepOne™ Plus Real-Time PCR System (Applied Biosystems; please see supplemental Figure S2). The 20 μl reaction mixture included a cDNA template corresponding to 20 ng of the original total RNA. While running the polymerization reaction, the real-time PCR system measured the cycle threshold values for each standard sample, and created a standard curve for each isoform by plotting cycle threshold values versus the log value of the transcript copy number. Using the regression equations calculated by the system software, the transcript copy number for each isoform in each unknown sample was calculated. Each was normalized by the value for GAPDH and then presented as an absolute copy number per 1000 copies of GAPDH transcript.

Statistical analyses

Expression levels of APP isoform transcripts were analyzed by unpaired, two-tailed Student's t-test. Plasma insulin concentrations and adipokine expression levels were log transformed when necessary to achieve a normal distribution (Lee et al. 2003). Simple linear regression was used to determine relationships between gene expression and metabolic parameters. A p-value less than .05 was considered significant. Data are presented as mean ± STDEV, except where noted.

Results

Increased expression of each of the APP isoforms in SAT of mice fed HFD

Absolute quantitative standards for each APP isoform transcript and GAPDH amplified with high fidelity and reproducibility; mean r^2 for standard curves of all APP isoforms and GAPDH were greater than 0.99 (please see supplemental Figure S3). Applying AQ-PCR with an absolute standard curve, mRNA expression level of each APP isoform was measured in abdominal SAT obtained from mice fed either an ND or HFD from the age of 6 weeks until the age of 16, 26, 36, 47, or 77 weeks. Transcript copy number of each APP isoform in each sample was normalized by the value for GAPDH, and then presented as an absolute copy number per 1000 copies of GAPDH. Transcript levels of all three major APP isoforms (APP770, APP 751, and APP695) in SAT were significantly increased in almost all HFD groups compared to that in age-matched ND mice (Figure 2).

Increasing APP transcript levels in SAT correlate with adipokine expression and plasma insulin levels

Linear regression analysis was carried out to determine the relationship between expression levels of each APP isoform in SAT and body weight, plasma insulin concentration, and expression levels of adipokines (IL-6, TNFα, CCL2) in SAT. Results showed that total transcript copy numbers of all three major APP isoforms (APP770 + APP751 + APP695) were significantly correlated with body weight ($R = 0.434$, $p < .001$) and SAT gene expression levels of TNFα, IL-6, and CCL2 ($R = 0.325$, $p < .01$; $R = 0.34$, $p < .01$; and $R = 0.655$, $p < .001$, respectively). Increasing transcript copy number of each APP770 and APP695 also significantly correlated with higher non-fasting plasma insulin concentrations ($R =$

Table 2. Sequences of primer and probe of custom TaqMan® gene expression assays for absolute quantification real-time PCR.

Assay	Amplicon size	Forward primer sequence[a]	Reverse primer sequence[a]	Probe sequence[a]
APP770	92bp	agtccgtggaggaggtggtc	tgtcgtgggaagtttatcag	ttgacacggaagagtactg
APP751	93bp	ccattctttacggcggatgt	tgtcgtgggaaacacgctg	ttgacacggaagagtactg
APP695	131bp	aggtggtccgagttccca	tcggtgcttggcttccag	acgagaacgagcatgc
GAPDH	110bp	ttgtcagcaatgcatcctgc	agtgatggcatggactgtgg	cctgccaagtatgatgac

[a]All sequences are listed from 5′ to 3′.

0.462, $p < .001$ and $R = 0.419$, $p < .001$, respectively, Figure 3(A) and (C)) and gene expression levels of CCL2 ($R = 0.667$, $p < .001$ and $R = 0.595$, $p < .001$, respectively, Figure 3(B) and (D)). These associations suggest that diet-induced obesity increased SAT expression of APP isoforms, which is associated with increased levels of insulin and adipokines, which may result in developing systemic metabolic abnormalities.

Ratios of APP isoforms in SAT were altered in obesity and aging and correlated with plasma glucose levels

Since APP alternative splicing and isoform ratios have been shown to play a role in the development of Aβ plaques and AD (Tharp et al. 2012; Alam et al. 2014; Love et al. 2015), we analyzed the expression ratios of APP isoforms in SAT. Results showed that APP695 expression in SAT was significantly increased with aging in both mice groups of ND (77 vs. 47 weeks, 96.2 ± 38.4 vs. 35.4 ± 17.5, $p < .001$) and HFD (77 vs. 47 weeks, 213.1 ± 48.5 vs. 68.9 ± 31.8, $p < .001$, Figure 2 and Table 3). Therefore, the ratios of transcript copy number of KPI-containing isoforms (APP-KPI, APP770 + APP751) to that of APP695 were gradually decreased with aging after the age of 26 weeks (Table 3). Since APP695 expression in SAT was significantly increased by HFD feeding in all age groups ($p < .05$, Figure 2) and dramatically increased in mice at 77 weeks of age compared to younger mice ($p < .001$, Figure 2), the ratio

(APP-KPI/APP695) was the lowest in mice fed a HFD until the age of 77 weeks (1.99 ± 0.3, Table 3).

In addition, linear regression analysis showed that the ratios of transcript copy number of APP770 or APP-KPI to that of APP695 were correlated with plasma glucose concentration ($R = 0.314$, $p < .01$ and $R = 0.323$, $p < .01$, respectively, Figure 4).

Change in transcript copy number of APP770 in SAT of TZD-treated obese mice

By AQ-PCR, transcript copy numbers of APP isoforms were measured in SAT from mice treated with TZD ($n = 10$) or vehicle ($n = 8$). In the TZD-treated mice, APP770 copy number was significantly decreased in SAT compared to control mice treated with vehicle only (230.7 ± 64.0 vs. 140.6 ± 43.7, $p < .01$, Figure 5). APP751 tended to be decreased in TZD-treated mice, but the difference was not statistically significant. However, no differences were found in APP695 copy numbers between two mice groups. These data suggest that TZD treatment affects KPI-containing peripheral-type APP isoforms but not the central-type APP isoform.

Discussion

In this study, AQ-PCR was developed for measuring transcript copy numbers of three major APP isoforms. By using a standard curve sample in copy number/volume
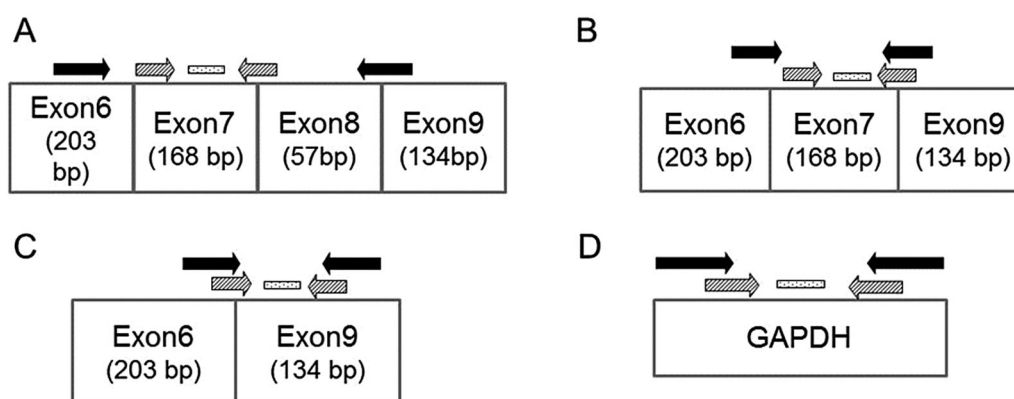

Figure 1. Schematic diagram showing the positions of primers (solid arrows) for standard curves samples, and primers (dashed arrows) and probes (dotted bars) for AQ-PCR for each APP isoform and GAPDH. (A) APP770, (B) APP751, (C) APP695, (D) GAPDH.
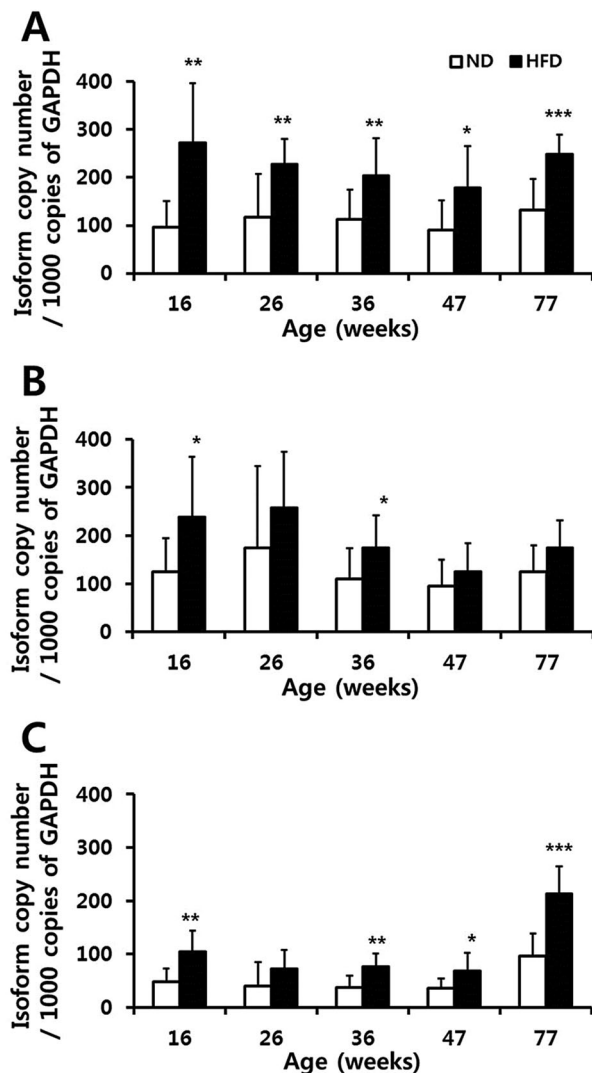
Figure 2. Transcript copy number of APP770 (A), APP751 (B), and APP695 (C) per 1000 mRNA transcript copies of GAPDH in SAT of C57BL/6 mice fed either a ND or HFD until 16, 26, 36, 47, or 77 weeks of age. *$p < .05$, **$p < .01$, ***$p < .001$ between mice on ND and HFD.

concentration for each APP isoform, the expression level of each of APP isoform in mouse SAT was quantified and normalized to that of GAPDH, and then presented as an absolute copy number per 1000 copies of GAPDH.

Although a great deal is known about neural APP and Aβ, APP is also widely expressed in peripheral tissues from skin, intestinal epithelia, and skeletal muscle, as well as leukocytes, platelets, pancreas, and adipose tissue (Joachim et al. 1989; Bush et al. 1990; Kuo et al. 2000; Hansel et al. 2003; Lee et al. 2008). However, the function and regulation of peripheral APP is not yet fully understood.

Several studies have demonstrated altered APP isoform ratios in platelets of AD patients and a correlation of platelet isoforms with the progression of clinical

symptoms and severity of cognitive loss in AD patients, suggesting the possibility that abnormal APP processing in the brain may be reflected in the periphery, thus suggesting it could serve as a diagnostic marker (Bush & Tanzi 1998; Di Luca et al. 1998).

Altered APP expression levels and aberrant processing was also observed in lymphoblastoid cells from subjects with familial AD, in parallel with increased expression of proinflammatory cytokines (Matsumoto & Fujiwara 1993). These data are similar to our previous observation that APP was increased in adipocytes/adipose tissue of obese individuals and mice and was correlated with gene expression profiles of proinflammatory cytokines (Lee et al. 2008; Jeong et al. 2014). In the current study, using a refined method for absolute quantitative analysis of the three major APP isoforms, we found significantly increased expression for all of three major APP isoforms in SAT of HFD-induced obese mice compared to age-matched control mice fed a ND. Expression levels of each isoform were correlated with adipokine expression and plasma levels of glucose. Collectively, these data suggest that peripheral changes in APP expression may be related to the progression of AD and inflammation and glucose metabolism in the periphery.

Further examination of isoform expression showed increased expression of the neuronal type APP isoform (APP695) in SAT of older mice fed either a ND or HFD, resulting in a decreasing ratio of APP-KPI to APP695 with aging. Therefore, the ratio (APP-KPI/APP695) was the lowest in 77-week-old mice. As documented previously (Karambataki et al. 2014), APP alternative splicing can be influenced by both the aging process and/or environmental factors, such as a HFD or obesity. By treating TZD to HFD-induced obese and insulin-resistant mice, we found that APP770 copy number was significantly decreased in SAT compared to control mice treated with vehicle only, whereas no differences were found in APP695 copy numbers between the two mice groups. In addition, linear regression analysis showed that the ratios of transcript copy number of APP770 or APP-KPI to that of APP695 correlated with plasma glucose concentration, suggesting that altered ratios of APP isoforms were related to systemic glucose metabolism and insulin sensitivity. These results suggest that not only APP expression but also expression ratios of APP isoforms in peripheral tissues may be related to aging and glucose metabolism and insulin sensitivity in the entire body and in the periphery.

Enzyme secretases have been known to have important roles in APP processing to Aβ and in AD pathogenesis. In our previous studies, we have demonstrated that secretases were expressed in adipose tissue. Although most of secretase genes were not differentially
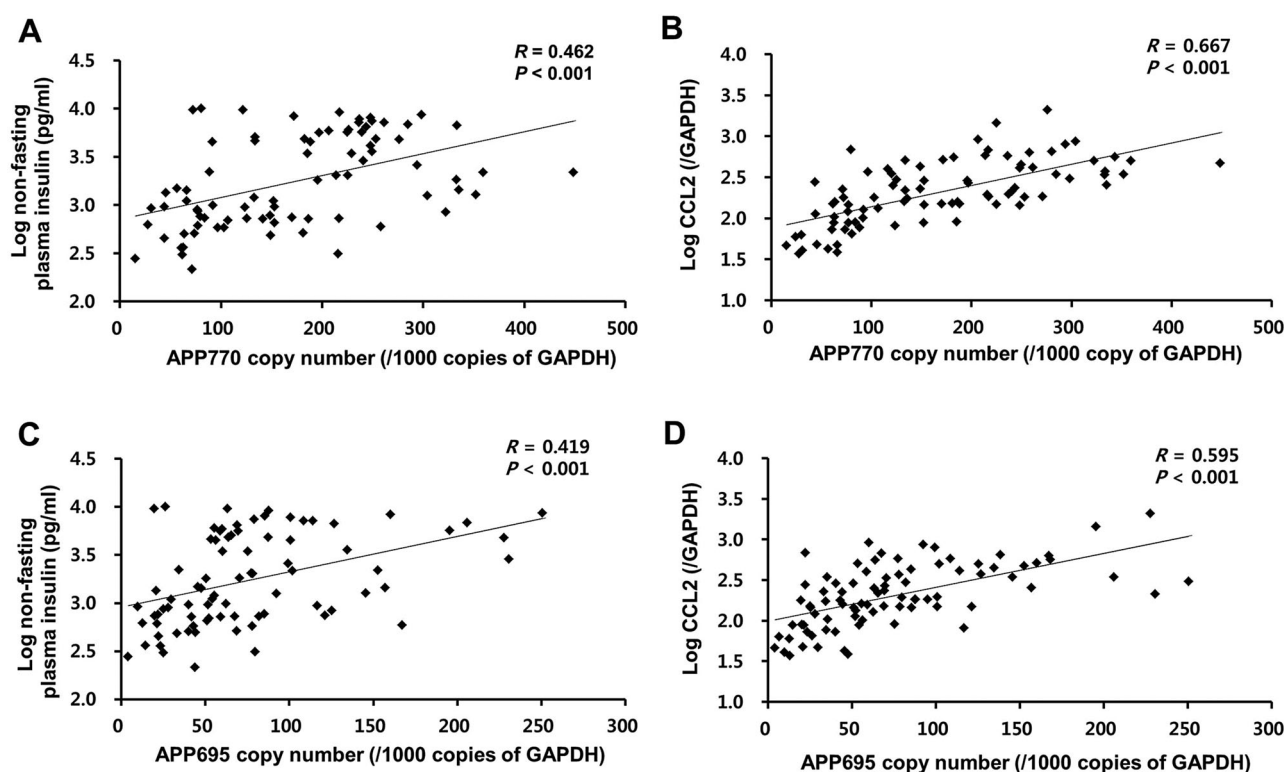
Figure 3. Transcript copy number of APP770 and APP695 (per 1000 mRNA transcript of GAPDH) in SAT correlated with non-fasting plasma insulin levels (A and C) and log expression level of CCL2 in SAT (B and D) of C57BL/6 mice fed either a ND or HFD until the age of 16, 26, 36, 47, or 77 weeks.

expressed with obesity, those expression data imply that the adipocyte/adipose tissue is equipped with the requisite enzymatic machinery for processing APP to its pathogenic cleavage products, Aβ40 and Aβ42 (Lee et al. 2008; Tharp et al. 2016). Additionally, in this study, mRNA expression levels of β-secretase-1 (BACE1), a representative secretase, were measured by relative qPCR to see the effect of long-term HFD feeding. The results did not show a noteworthy feature and are consistent to our previous BACE1 expression data in human adipose tissue (supplemental Figure S4).

The presence of cis-elements and the tissue-specific expression of trans-acting factors, such as the RNA-binding protein fork head box for APP (RBFox) (Alam et al. 2014), regulate overall alternative splicing patterns (Qian & Liu 2014; Stilling et al. 2014). There is still little known about factors contributing to the alternative splicing of the APP gene in obesity and aging, and further research is needed to examine if RBFox proteins play a

role in this process (Love et al. 2015). Our results suggest that HFD feeding and obesity is likely to alter APP alternative splicing, which could be affected by trans-acting factors. Elucidating the mechanism of APP alternative splicing in adipose tissue with obesity and the exact role that alternative splicing events play in enhancing the production of Aβ could contribute to the development of new drug targets for preventing obese-related AD and other complications of obesity.

In summary, this study developed an absolute quantification method to measure absolute copy numbers of major APP isoforms, and demonstrated that APP isoforms were increased in mouse adipose tissue with obesity and the ratios of APP isoforms were altered with aging. In addition, isoform expressions were correlated with *in vivo* measures of glucose metabolism and a proinflammatory pattern of adipokine expression in adipose tissue. We demonstrated that treatment of insulin sensitizer could reduce the increased expression

Table 3. Ratios of transcript copy number of KPI-containing isoforms (APP-KPI, APP770 + APP751) to that of APP695.

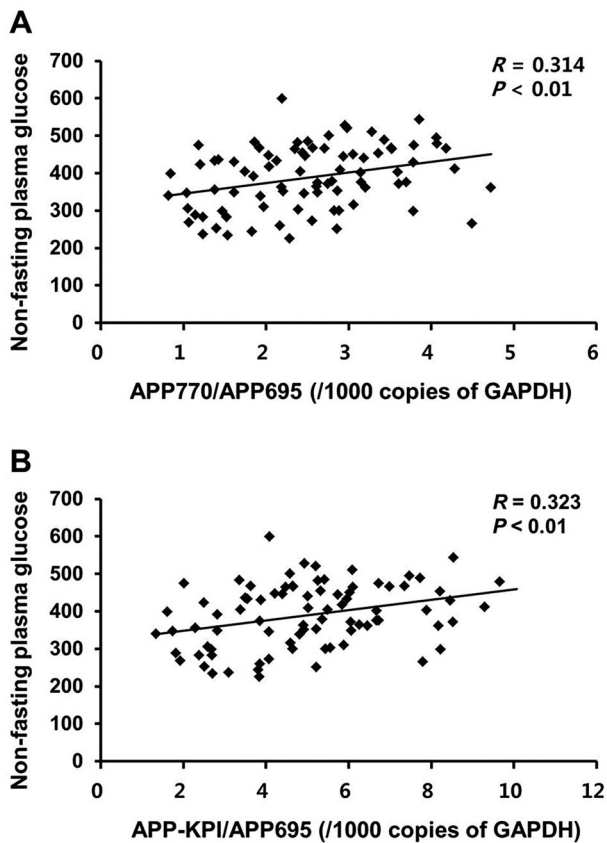| Ratio	Diet	Age at sacrifice (weeks)				
		16	26	36	47	77
(APP770 + APP751)/APP695	ND	4.61 ± 1.0	7.21 ± 1.8	5.99 ± 1.4	5.22 ± 1.7	2.68 ± 0.2
	HFD	4.88 ± 0.9	6.63 ± 1.4	4.95 ± 1.4	4.43 ± 1.3	1.99 ± 0.3

Figure 4. Correlation of non-fasting plasma glucose levels with ratios of transcript copy number of APP770 (A) and APP-KPI (B) to that of APP695 in SAT of C57BL/6 mice fed either a ND or HFD until 16, 26, 36, 47, or 77 weeks of age.

of the APP770 isoform. To our knowledge, this study is the first to measure the absolute copy number of APP isoforms in adipose tissue by AQ-PCR. The method presented is simple, and accurately compares expression levels of each APP isoform from the same sample. It can be implemented in a standardized fashion, allowing APP isoform expression data to be compared between
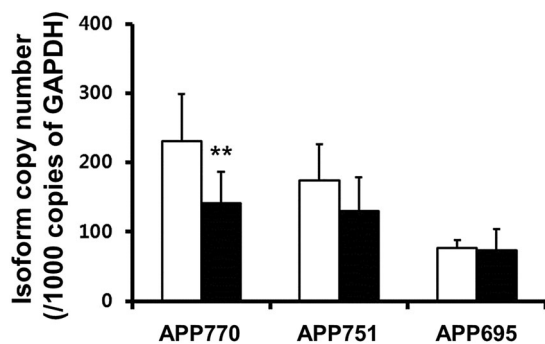

Figure 5. Transcript copy number of APP isoforms (per 1000 transcript copies of GAPDH) in SAT from TZD treated mice (closed bars) and control mice treated with vehicle only (open bars). **$p < .01$.

experiments and across studies conducted by independent research groups. Understanding the biology and the potential importance of peripheral tissues of APP regulation and the expression of specific isoforms is critical to unraveling the pathology of APP-related abnormalities, such as AD. Finally, the relationship between adipose tissue expression of APP and Aβ peptides and risk for AD are not well known, and will require long-term studies to address.

Disclosure statement

No potential conflict of interest was reported by the authors.

Funding

References

Alam S, Suzuki H, Tsukahara T. 2014. Alternative splicing regulation of APP exon 7 by RBFox proteins. Neurochem Int. 78:7–17.

Barrachina M, Dalfo E, Puig B, Vidal N, Freixes M, Castano E, Ferrer I. 2005. Amyloid-beta deposition in the cerebral cortex in dementia with Lewy bodies is accompanied by a relative increase in AbetaPP mRNA isoforms containing the Kunitz protease inhibitor. Neurochem Int. 46:253–260.

Bush AI, Martins RN, Rumble B, Moir R, Fuller S, Milward E, Currie J, Ames D, Weidemann A, Fischer P, et al. 1990. The amyloid precursor protein of Alzheimer's disease is released by human platelets. J Biol Chem. 265:15977–15983.

Bush AI, Tanzi RE. 1998. Alzheimer disease-related abnormalities of amyloid beta precursor protein isoforms in the platelet: the brain's delegate in the periphery? Arch Neurol. 55:1179–1180.

Di Luca M, Pastorino L, Bianchetti A, Perez J, Vignolo LA, Lenzi GL, Trabucchi M, Cattabeni F, Padovani A. 1998. Differential level of platelet amyloid beta precursor protein isoforms: an early marker for Alzheimer disease. Arch Neurol. 55:1195–1200.

Hansel DE, Rahman A, Wehner S, Herzog V, Yeo CJ, Maitra A. 2003. Increased expression and processing of the Alzheimer amyloid precursor protein in pancreatic cancer may influence cellular proliferation. Cancer Res. 63:7032–7037.

Hardy J, Selkoe DJ. 2002. The amyloid hypothesis of Alzheimer's disease: progress and problems on the road to therapeutics. Science. 297:353–356.

Jeong JI, Kim J, Kim KM, Choi I, Pratley RE, Lee YH. 2014. Altered gene expression of amyloid precursor protein in the adipose tissue and brain of obese mice fed with long-term high-fat

diet and streptozotocin-induced diabetic mice. Anim Cells Syst. 18:219–227.

Joachim CL, Mori H, Selkoe DJ. 1989. Amyloid beta-protein deposition in tissues other than brain in Alzheimer's disease. Nature. 341:226–230.

Karambataki M, Malousi A, Kouidou S. 2014. Risk-associated coding synonymous SNPs in type 2 diabetes and neurodegenerative diseases: genetic silence and the underrated association with splicing regulation and epigenetics. Mutat Res. 770:85–93.

Kim J, Jeong JI, Kim KM, Choi I, Pratley RE, Lee YH. 2014. Improved glucose tolerance with restored expression of glucose transporter 4 in C57BL/6 mice after a long period of high-fat diet feeding. Anim Cells Syst. 18:197–203.

Kuo YM, Kokjohn TA, Watson MD, Woods AS, Cotter RJ, Sue LI, Kalback WM, Emmerling MR, Beach TG, Roher AE. 2000. Elevated abeta42 in skeletal muscle of Alzheimer disease patients suggests peripheral alterations of AbetaPP metabolism. Am J Pathol. 156:797–805.

Lee YH, Martin JM, Maple RL, Tharp WG, Pratley RE. 2009. Plasma amyloid-beta peptide levels correlate with adipocyte amyloid precursor protein gene expression in obese individuals. Neuroendocrinology. 90:383–390.

Lee YH, Nair S, Rousseau E, Allison DB, Page GP, Tataranni PA, Bogardus C, Permana PA. 2005. Microarray profiling of isolated abdominal subcutaneous adipocytes from obese vs non-obese pima Indians: increased expression of inflammation-related genes. Diabetologia. 48:1776–1783.

Lee YH, Tharp WG, Maple RL, Nair S, Permana PA, Pratley RE. 2008. Amyloid precursor protein expression is upregulated in adipocytes in obesity. Obesity. 16:1493–1500.

Lee YH, Tokraks S, Pratley RE, Bogardus C, Permana PA. 2003. Identification of differentially expressed genes in skeletal muscle of non-diabetic insulin-resistant and insulin-sensitive pima Indians by differential display PCR. Diabetologia. 46:1567–1575.

Ling Y, Morgan K, Kalsheker N. 2003. Amyloid precursor protein (APP) and the biology of proteolytic processing: relevance to Alzheimer's disease. Int J Biochem Cell Biol. 35:1505–1535.

Love JE, Hayden EJ, Rohn TT. 2015. Alternative splicing in Alzheimer's disease. J Parkinsons Dis Alzheimers Dis. 26. doi:10.13188/2376-922X.1000010

Matsui T, Ingelsson M, Fukumoto H, Ramasamy K, Kowa H, Frosch MP, Irizarry MC, Hyman BT. 2007. Expression of APP pathway mRNAs and proteins in Alzheimer's disease. Brain Res. 1161:116–123.

Matsumoto A, Fujiwara Y. 1993. Aberrant proteolysis of the beta-amyloid precursor protein in familial Alzheimer's disease lymphoblastoid cells. Eur J Biochem. 217:21–27.

Nair S, Lee YH, Rousseau E, Cam M, Tataranni PA, Baier LJ, Bogardus C, Permana PA. 2005. Increased expression of inflammation-related genes in cultured preadipocytes/stromal vascular cells from obese compared with non-obese pima Indians. Diabetologia. 48:1784–1788.

Qian W, Liu F. 2014. Regulation of alternative splicing of tau exon 10. Neurosci Bull. 30:367–377.

Stilling RM, Benito E, Gertig M, Barth J, Capece V, Burkhardt S, Bonn S, Fischer A. 2014. De-regulation of gene expression and alternative splicing affects distinct cellular pathways in the aging hippocampus. Front Cell Neurosci. 8:373. doi:10.3389/fncel.2014.00373

Tharp WG, Gupta D, Smith J, Jones KP, Jones AM, Pratley RE. 2016. Effects of glucose and insulin on secretion of amyloid-beta by human adipose tissue cells. Obesity. 24:1471–1479.

Tharp WG, Lee YH, Greene SM, Vincellete E, Beach TG, Pratley RE. 2012. Measurement of altered AbetaPP isoform expression in frontal cortex of patients with Alzheimer's disease by absolute quantification real-time PCR. J Alzheimers Dis. 29:449–457.

Zhao YJ, Han HZ, Liang Y, Shi CZ, Zhu QC, Yang J. 2015. Alternative splicing of VEGFA, APP and NUMB genes in colorectal cancer. World J Gastroenterol. 21:6550–6560.